

Selected Paper

Novel Functional Groups with Fine-Controlled Metal Assembling Function

Kimihisa Yamamoto,* Masayoshi Higuchi, Atsushi Kimoto, Takane Imaoka, and Kiriko Masachika

Department of Chemistry, Faculty of Science & Technology, Keio University, Yokohama 223-8522

Received July 2, 2004; E-mail: yamamoto@chem.keio.ac.jp

Half-substituted dendritic phenylazomethine dendrimers with various substituents (**Half-DPA-X G*n***, where *n* is the generation number) were synthesized in order to elucidate the electron gradients in the dendrons by complexation with metal ions. Along with the change in the UV–vis spectra, the isosbestic point shifted about 11 nm from 371 to 360 nm. The number of added equivalents of $SnCl_2$ required to induce a shift was in agreement with the number of the imine sites present in each layer of **Half-DPA-H G4**. The degree of the electron gradient in the phenylazomethine monodendrons, **Half-DPA**s, was estimated via titration with trifluoroacetic acid. We found drastic differences in the basicity of the imine sites; the basicity of the core imines is higher than that of the more peripheral imines. The stepwise complexation behavior is thermodynamically controlled from the core to terminal imines in **Half-DPA-H**. Furthermore, **Half-DPA G4** with various substituents possesses the same electron gradients in the dendron, so the complexation behavior with metal ions is the same.

Dendrimers[1] are nanosized macromolecules with a regular tree-like array of units, providing gradients in the branch density from the interior to the exterior which direct the transfer of charge and energy from the dendrimer periphery to its core.[2] We can move to the next stage of advanced molecular design by utilizing these molecular funnels in electric and/or optic applications, such as a photovoltaic cell and an electroluminescence device.[3] These electro-optical devices possess the sequential HOMO/LUMO energy gradients of a fixed vector within a device with the multi-layered structure and lower energy barriers. Another important aspect of a dendritic structure with some peripheral units is an energy harvesting, resulting in a highly efficient emission.[4] We have recently synthesized the phenylazomethine (phenyliminomethane) dendrimer, and found that the tin ions, Sn^{2+}, are coordinated on the imine groups in a stepwise fashion.[5] This complexation behavior was supported by UV–vis spectroscopy, ^{1}H NMR measurements and TEM, confirming the expansion of the molecular size due to complexation. This behavior reflects a gradient in the electron density associated with the imine groups, and it should be possible to control the number and location of the metal ions incorporated into the dendrimer structures. This unique complexation might find use in creating tailored catalysts or building blocks for advanced materials.

For our next strategy, the dendron, which is a dendrimer compound, should be employed in order to overcome any synthetic difficulties. Moreover, the dendrons expand the possibilities for advanced materials, for example, dendronized polymer,[6] surface modification of electrode or metal cluster.[7] Half-substituted dendritic phenylazomethine dendrimers with various substituents (**Half-DPA-X G*n***, where *n* is the generation number) were synthesized in order to elucidate the electron gradients in the dendrons by complexation with metal ions. We estimated the basicity within the phenylazomethine dendron by profiling the change in the UV–vis spectra. We found a unique behavior in which a metal ion is stepwise assembled during each generation of the dendron.

Results and Discussion

Synthesis of the DPA Dendrons and Half-DPAs. Dendritic phenylazomethine (**DPA**) dendrons G*n* ($n = 1$–4) were synthesized via dehydration of aromatic ketones with aromatic amines in the presence of titanium tetrachloride, and then isolated by silica gel column chromatography.[8] **Half-DPA-H G1**, **G2**, **G3**, and **G4** (Fig. 1) were obtained by the dehydration of benzophenone, dendrons G2, G3, and G4[8] (ketones) with aniline, and isolated in 92, 90, 89, and 80% yields, respectively. This dehydration efficiently proceeded, and the yields are significantly higher than those reported in the dehydration of DPA dendrons and *p*-phenylenediamine,[5] because aniline derivatives can be added in excess with a lower steric hindrance at the last step. The isolated **Half-DPA**s were identified by ^{1}H and ^{13}C NMR spectroscopies, elemental analysis, and matrix-assisted laser desorption/ionization time-of-flight mass spectroscopy (MALDI-TOF MS).

UV–Visible Spectra of Half-DPAs with $SnCl_2$.[9] The spectra of **Half-DPA-H G4** gradually changed (Fig. 2a), with an isosbestic point at 371 nm up to the addition of 1 equivalent (molar amount) of $SnCl_2$. The isosbestic point then shifted upon the further addition of $SnCl_2$, and appeared at 368 nm between 1 and 3 equivalents. With the addition of between 3 and 7 equivalents of $SnCl_2$, an isosbestic point appeared at 363 nm, moving to 360 nm when between 7 and 15 equivalents were added (Fig. 2b). Overall, the isosbestic point shifted about 11 nm from 371 to 360 nm, and the number of added equivalents of $SnCl_2$ required to induce a shift was in agreement with the number of imine sites present in each layer of **Half-DPA-H G4**. From a kinetic standpoint, complexation of the terminal imines of the dendrimer is expected to occur first. However, the titration results suggest that, on the time scale of our obser-

Published on the web February 11, 2005; DOI 10.1246/bcsj.78.349

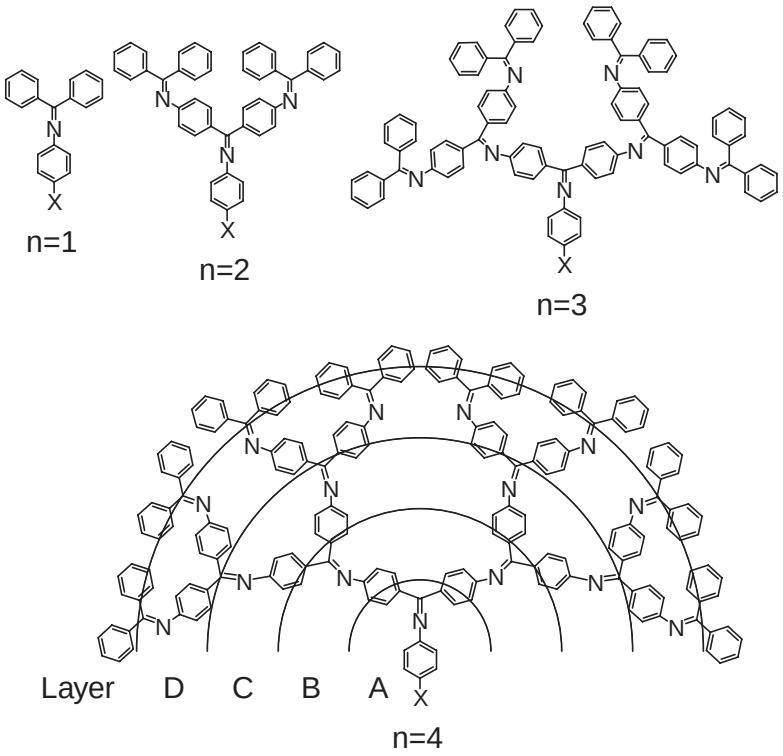

Fig. 1. Chemical structures of the **Half-DPA-X G*n*** (n = 1–4) and four imine layers.

vations, the process is thermodynamically controlled and proceeds in a stepwise fashion from the core imines to the terminal imines of **Half-DPA-H G4** (Fig. 2c). A similar stepwise complexation was previously reported in phenylazomethine dendrimers,[5] and was also observed in **Half-DPA-H G2** (352 and 349 nm for 0–1 and 1–3 equivalents of $SnCl_2$, respectively) and in **Half-DPA-H G3** (362, 358, and 351 nm upon adding 0–1, 1–3, and 3–7 equivalents).[10] These results further supported the idea that metal ions are incorporated in a stepwise fashion, first filling the shells close to the dendrimer core and then progressively filling the more peripheral shells. The spectral changes accompanying the addition of $SnCl_2$ to the linear phenylazomethine dimer and trimer[5a] resulted in the appearance of only one isosbestic point in each case. This behavior shows that the complexation between $SnCl_2$ molecules and the imine sites is random. Therefore, these observations suggest that the stepwise complexation behavior in DPAs does not reflect changes in the basicity of the imine groups induced by complexation at the neighboring imine groups. If that were the case, we would also expect to see stepwise complexation when titrating the linear oligomers. Also, this stepwise behavior has been supported by several other measurements such as ^{1}H NMR measurement and direct observation of the molecular size by TEM.[5a,d]

Drastic differences in the basicity of the imines results in the stepwise complexation behavior of the **Half-DPA-H G4**. The experimental observations suggest that the basicity of the core imine is higher than that of the more peripheral imines. These conclusions are further supported by determination of the complexation constants K of each generation using UV–visible spectroscopy. However, the K values obtained from the $SnCl_2$ titration are enormous, so the method is unsuitable for the quantitative evaluation of the degree of the electron gradient present in the **Half-DPA**s.

Basicity of the Imine Units in Each Generation of the Half-DPAs. For the quantitative evaluation, we have to know how much difference between neighboring complexation constants K is required for the stepwise complexation. To answer this question, we first tried to make a theoretical model of the multi-equilibrium system. For the first assumption, the electronic effect of preceding complexation at the other free imines were neglected. This is justified because the stepwise complexation from the core side was clearly observed. If the effect was not negligible, the coordinating metals should be dispersed, because one complexation lowered the constants of neighboring imines through bond electron withdrawing. Therefore, we can use the simplest four-equilibrium model expressed below.

$$[A] + [H^+] \rightleftharpoons [AH^+]: K_a \quad (1)$$

$$[B] + [H^+] \rightleftharpoons [BH^+]: K_b \quad (2)$$

$$[C] + [H^+] \rightleftharpoons [CH^+]: K_c \quad (3)$$

$$[D] + [H^+] \rightleftharpoons [DH^+]: K_d. \quad (4)$$

In these equations, protonations by H^+ are assumed instead of complexations by $SnCl_2$. The complexation reactions by $SnCl_2$ can also treated by the same procedures. [A]–[D] and [AH^+]–[DH^+] represent the unit concentrations of free base imines and coordinated imines in four layers (here we assumed that "A" is the first layer nearest to the focal point), respectively. The calculation method described in the experimental section can predict the shift of the isosbestic point on the addition of H^+, if each coordination constant (K_a–K_d) and the maximum absorption wavelengths (λ^0) of each chromophore (A–D and AH^+–DH^+) are given.

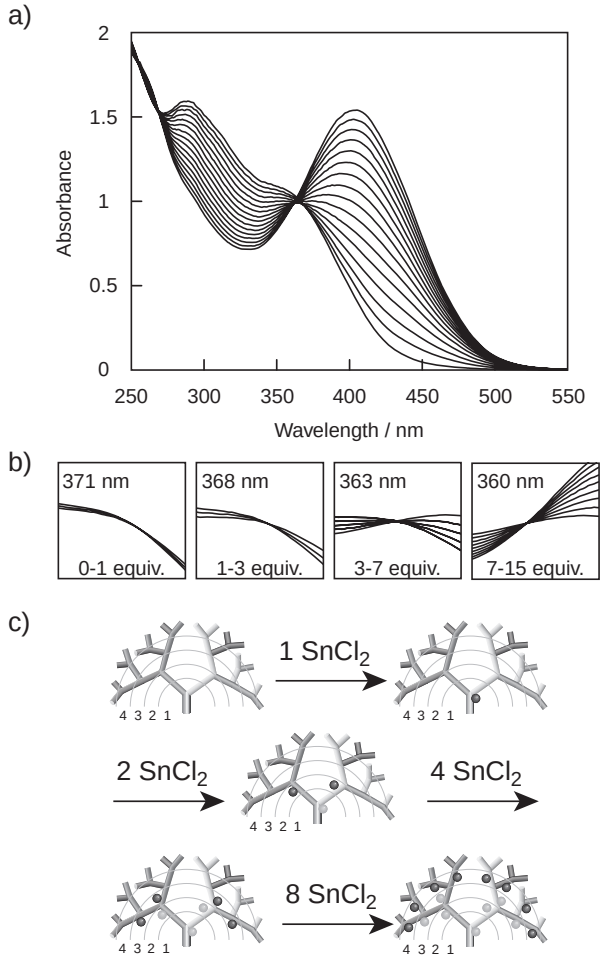

Fig. 2. a) UV–vis spectral changes in **Half-DPA-H G4** upon the stepwise addition of $SnCl_2$ to $CH_3CN/CH_2Cl_2 = 1/1$, b) enlargements showing isosbestic points during complexation with $SnCl_2$, and c) schematic representation of stepwise radial complexation of **Half-DPA-H G4** with $SnCl_2$.

Table 1. Equilibrium Constants of Protonations to Each Imine Site

K_N/M^{-1}	(a)	(b)	(c)
K_a	10^{10}	10^7	10^7
K_b	10^8	10^6	10^7
K_c	10^6	10^5	10^7
K_d	10^4	10^4	10^7

Secondly, we tried to apply the defined model to three example cases. For each case, the concentration of the dendrimer (here we assume **Half-DPA-G4**) was set to 2×10^{-5} M, so that the initial unit concentrations of imines (defined as $[A]_0$, $[B]_0$, $[C]_0$, and $[D]_0$) become 2×10^{-5}, 4×10^{-5}, 8×10^{-5}, and 16×10^{-5} M, respectively. When the complexation constants K_N (N = A–D) are the values listed in Table 1 (a, b and c), the concentration profiles are calculated as shown in Fig. 3. If the λ^0 values are given as in Table 2, the variation of the isosbestic point λ_{iso} can be calculated as shown in Fig. 4 from the concentration profiles in Fig. 3a. The results

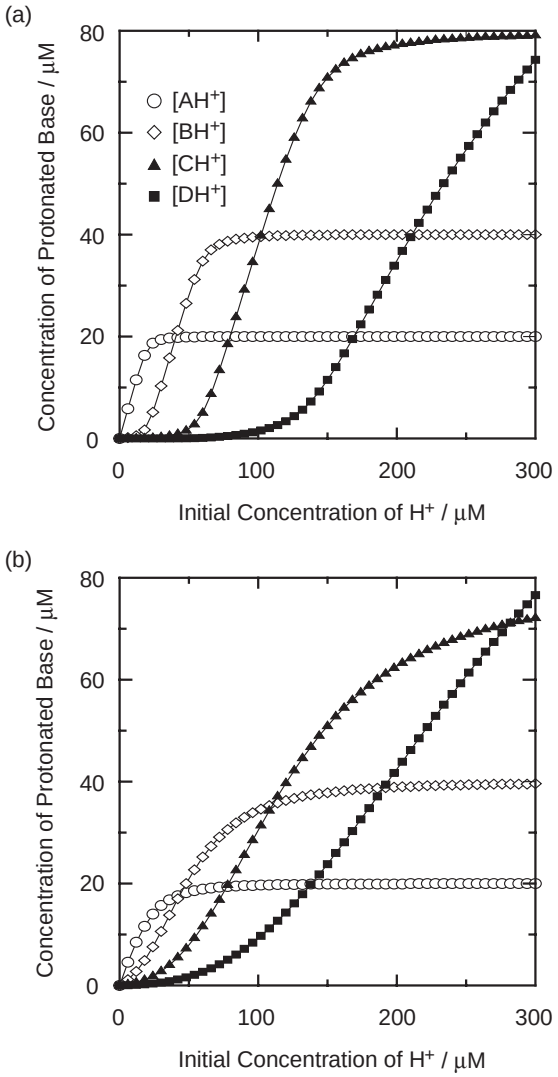

Fig. 3. Calculated concentration profiles of protonated imines upon addition of H^+ when K_N are the values in Table 1, $[A]_0 = 2.0 \times 10^{-5}$ M, $[B]_0 = 4.0 \times 10^{-5}$ M, $[C]_0 = 8.0 \times 10^{-5}$ M, $[D]_0 = 1.6 \times 10^{-4}$ M.

Table 2. Assumed Peak Wavelength for the Simulation of Isosbestic Point

N	λ^0_N/nm	λ^0_{NH}/nm
A	336	406
B	333	403
C	328	398
D	325	395

clearly show that at least 100 times difference between neighboring complexation constants is required to observe the stepwise shift of isosbestic point. If the difference is set to 10 times, the shift would be continuous. Therefore, in any experimental case, the complexation constant of inner imines should be 100 times larger than that of the neighboring outer imines.

To apply these methods to the experiment, we have to decide λ^0 values experimentally. The λ^0 values could be practically obtained from the differential spectra of the UV–vis ab-

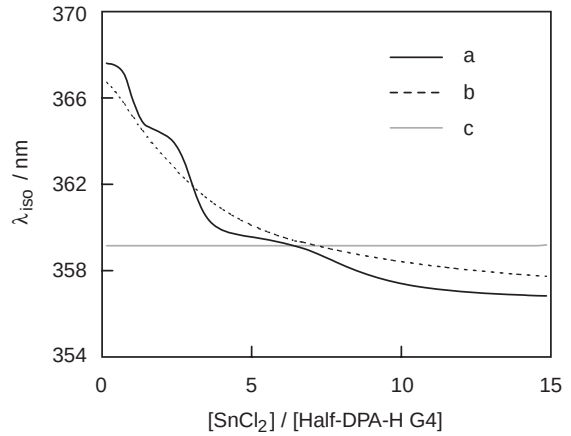

Fig. 4. The variation in the isosbestic point calculated from the peak wavelengths in Table 3 (a, b, and c) and concentration profiles in Fig. 3.

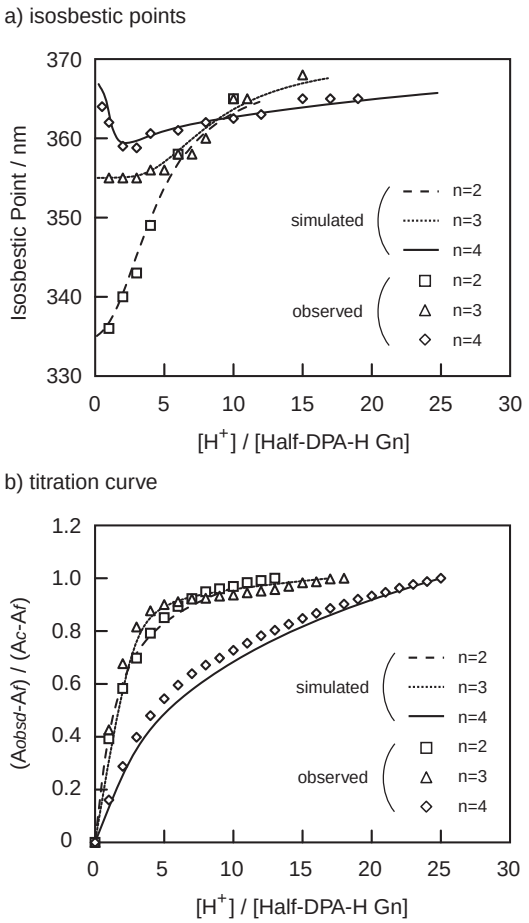

Fig. 5. Results of the simulations, a) isosbestic points and b) titration curve.

sorption when the K_N (N = A–D) values are different enough to discriminate the basicity of each imine by the proton titration. The spectral change during the addition of H^+ up to 1 molar amount reflects the chromophore of the free base and coordinated imine at the root nearest to the focal point. The wavelength of the negative valley in the differential spectrum

Table 3. Basicity [M^{-1}] of the Imine Units for Each Generation of **Half-DPA-H G*n***

n	A	B	C	D
1	1.1×10^3			
2	7.0×10^4	9.0×10^2		
3	1.3×10^7	2.0×10^5	1.0×10^3	
4	1.5×10^7	3.0×10^5	1.4×10^4	1.2×10^3

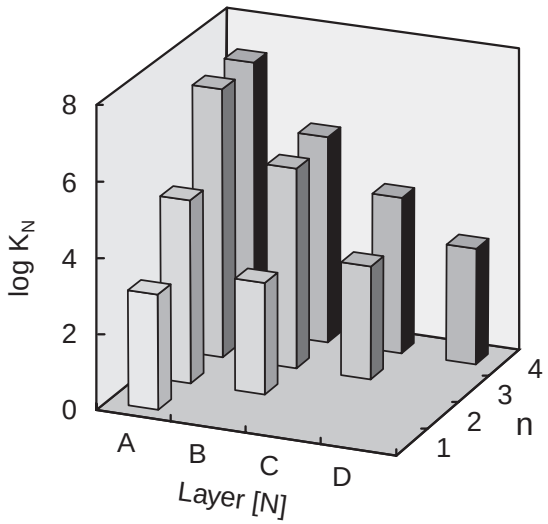

Fig. 6. Schematic representation of basicity within each layer of **Half-DPA G*n*** (n = 1–4).

is attributed to the $\lambda^0{}_A$ (maximum wavelength of free base chromophore), and the positive peak is attributed to the $\lambda^0{}_{AH}$ (maximum wavelength of coordinated chromophore), respectively. Similar analyses were performed on the next three generations to obtain $\lambda^0{}_B \sim \lambda^0{}_D$ and $\lambda^0{}_{BH} \sim \lambda^0{}_{DH}$. The expected isosbestic points are calculated for every equivalent of added H^+ using these parameters.

The systematic changes in the UV spectra were also recorded in dichloromethane with the addition of various concentrations of trifluoroacetic acid to **Half-DPA** solutions, instead of using $SnCl_2$, whereas the complexation constant K of that acid to the imines is relatively small. The values of K_N represent the complexation constant of the imines in each generation and are estimated by the curve fitting of two simulated curves; i.e., isosbestic point change and absorption change (Fig. 5). The basicity of the four imine units in each generation obtained from the simulation are listed in Table 3 and shown in Fig. 6. Here, the complexation constant K for the **Half-DPAs** indicates a downward electron gradient structure from the core to terminal phenylazomethines. In **Half-DPA-H G3** and **G4**, the basicity of the core imine proved to be extraordinarily large ($\sim 10^7$ M^{-1}). These values of the terminal branch imines are roughly of the same order ($\sim 10^3$ M^{-1}) as those of **Half-DPA-H G1** for all generations. From these simulations, the complexation constant should be larger than the outer phenylazomethines for the spectral changes with the stepwise isosbestic point. If the difference is about ten times, only a continuous change in the isosbestic points could be observed (Fig. 4). Indeed, this result calculated from the UV–vis spectral change proved that

the inner complexation constant for **Half-DPA-H** is over ten times larger than the values of the neighboring outer imines. We found drastic differences of the basicity in the phenylazomethine moiety; the basicity of the core imines is higher than those of the more peripheral imines.[11] This stepwise complexation process is thermodynamically controlled from the core to terminal imines in **Half-DPA-H**.

The complex formation constant K of $SnCl_2$ with **Half-DPA-H G1** was determined to be 9.5×10^4 M^{-1} in dichloromethane. The K value is 100 times greater than that of a proton. On the basis of this result, the formation constants of $SnCl_2$ with **Half-DPA-H G4** for each generation are postulated to be two orders of magnitudes greater than that of a proton.

Synthesis of the Half DPAs with Various Substituents. We also changed the core phenyl ring of **Half-DPA G4** to three other substituents: methoxyphenyl (X = MeO, Fig. 1), an electron-donating group, by dehydration of the G4 dendron with methoxyaniline; chlorophenyl, an electron-drawing group, by dehydration of the G4 dendron with chloroaniline (X = Cl, Fig. 1); and trifluoromethylphenyl, a strong electron-withdrawing group, by dehydration of the G4 dendron with trifluoromethylaniline (X = CF_3, Fig. 1).

When $SnCl_2$ was added to the **Half-DPA G4** carrying a methoxyphenyl core (**Half-DPA-MeO G4**), four isosbestic points appeared at 373, 366, 361, and 360 nm upon adding 0–1, 1–3, 3–7, and 7–15 equivalents of $SnCl_2$, respectively. When $SnCl_2$ was added to the **Half-DPA G4** carrying a chlorophenyl, a weak electron-drawing core (**Half-DPA-Cl G4**), four isosbestic points are observed in the same manner. These stepwise complexation behaviors resulted from the original electron gradients that did not change in these dendrons.

On the other hand, when $SnCl_2$ was added to the **Half-DPA G4** having a trifluoromethylphenyl core (**Half-DPA-CF_3 G4**), three isosbestic points appeared at 371, 365, and 363 nm upon adding 0–1, 1–3, and 3–15 equivalents of $SnCl_2$, respectively. This behavior suggested that the electron gradient between the third and fourth layers (C and D, Fig. 1) is cancelled by the strong electron-withdrawing substituent (Fig. 7).

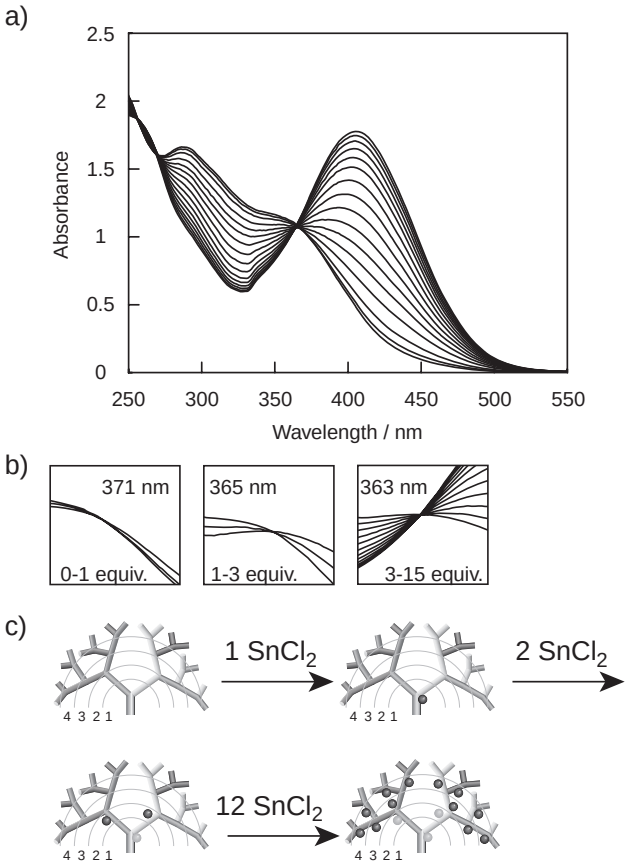

Fig. 7. a) UV–vis spectral changes in **Half-DPA-CF_3 G4** upon the stepwise addition of $SnCl_2$ to CH_3CN/CH_2Cl_2 = 1/1, b) enlargements showing isosbestic points during complexation with $SnCl_2$, and c) schematic representation of stepwise radial complexation of **Half-DPA-CF_3 G4** with $SnCl_2$.

Conclusion

In conclusion, the degree of the electron gradient in the phenylazomethine dendron, **Half-DPA**s, was estimated via titration with trifluoroacetic acid. We found drastic differences in the basicity of the imine sites; the basicity of the core imines is higher than that of the more peripheral imines. The stepwise complexation behavior is thermodynamically controlled from the core to terminal imines in **Half-DPA-H**. Furthermore, **Half-DPA G4** with various substituents possesses the same electron gradients in the dendron and shows the same complexation behavior with metal ions. We found a unique behavior in which a metal ion is stepwise assembled in each generation of the dendron on the basis of the dendron gradients. The electron gradients in the dendrons were able to be controlled by the introduction of various substituents.

Experimental

General. The NMR spectra were recorded using a JEOL JMN400 FT-NMR spectrometer (400 MHz) in $CDCl_3$ + TMS (internal standard) solution. The MALDI-TOF-Mass spectra were obtained using a Shimadzu/Kratos KOMPACT MALDI mass spectrometer (Positive mode, Matrix: Dithranol). The UV–vis spectra were recorded using a Shimadzu UV-3100PC spectrometer with a sealed quartz cell (optical path length: 1 cm). All chemicals were purchased from Aldrich, Tokyo Kasei Co., Ltd., and Kantoh Kagaku Co., Inc. (reagent grade) and were used without further purification.

General Procedure for the Synthesis of Half-DPA-X G*n*. $TiCl_4$ was dropwise added to a mixture of the aniline derivatives, the corresponding phenylazomethine dendron and DABCO in chlorobenzene. The addition funnel was then rinsed with chlorobenzene. The reaction mixture was heated in an oil bath at 125 °C for 30 min under N_2. The precipitate was removed by filtration. The filtrate was concentrated, and the pure product was isolated by silica gel column chromatography.

Half-DPA-H G1: The previous procedure was followed using 0.55 mL (6.0 mmol) of aniline, 0.91 g (5.0 mmol) of benzophenone (n = 1), 0.84 g (7.5 mmol) of DABCO, and 3.3 mL (30 mmol) of $TiCl_4$. The product was isolated by silica gel column chromatography using 7:1 hexane/ethyl acetate with 2% Et_3N as the eluent, yielding 1.18 g (92%). ^{1}H NMR (400 MHz, $CDCl_3$, TMS standard, 20 °C, ppm) δ 7.67 (t, J = 7.6 Hz, 1H), 7.31 (d, J = 7.6 Hz, 2H), 7.26 (t, J = 7.6 Hz, 1H), 7.18 (dd, J = 7.6, 7.6 Hz, 2H), 7.14 (dd, J = 7.6, 7.6 Hz, 2H), 7.13–7.06 (m, 5H), 6.53 (d, J = 7.6 Hz, 2H); ^{13}C NMR (100 MHz, $CDCl_3$, TMS

standard, 20 °C, ppm) δ 168.06, 151.08, 139.54, 136.08, 130.58, 129.39, 129.19, 128.43, 128.34, 128.07, 127.76, 123.02, 120.83; MALDI-TOF-Mass: 257.3 ($[M]^+$ Calcd for $C_{19}H_{15}N$: 257.1); Anal. Calcd for $C_{19}H_{15}N$: C, 88.68; H, 5.88; N, 5.44%. Found: C, 88.67, H, 5.59; N, 5.45%.

Half-DPA-H G2: The previous procedure was followed using 0.08 mL (9.25 mmol) of aniline, 0.050 g (0.93 mmol) of the G2 dendron, 0.16 g (1.4 mmol) of DABCO, and 0.6 mL (5.6 mmol) of $TiCl_4$. The product was isolated by silica gel column chromatography using from 7:1:1 to 4:1:1 hexane/ethyl acetate/chloroform with 2% Et_3N as the eluent, yielding 0.514 g (90%). ^1H NMR (400 MHz, $CDCl_3$, TMS standard, 20 °C, ppm) δ 7.73 (t, $J = 7.1$ Hz, 4H), 7.50 (d, $J = 8.3$ Hz, 2H), 7.47–7.38 (m, 6H), 7.30–7.13 (m, 10H), 7.02–6.92 (m, 2H), 6.90–6.85 (m, 2H), 6.72 (d, $J = 8.0$ Hz, 2H), 6.56 (d, $J = 2.4$ Hz, 2H), 6.54 (d, $J = 8.1$ Hz, 2H); ^{13}C NMR (100 MHz, $CDCl_3$, TMS standard, 20 °C, ppm) δ 168.73, 168.33, 167.74, 139.28, 135.78, 135.64, 134.59, 132.32, 130.83, 130.06, 129.97, 129.89, 129.37, 129.32, 129.25, 128.76, 128.58, 128.29, 127.73, 120.44; MALDI-TOF-Mass: 615.0 ($[M]^+$ Calcd for $C_{45}H_{33}N_3$: 615.3); Anal. Calcd for $C_{45}H_{33}N_3$: C, 87.77; H, 5.40; N, 6.82%. Found: C, 87.70; H, 5.42; N, 6.81%.

Half-DPA-H G3: The previous procedure was followed using 0.07 mL (0.80 mmol) of aniline, 0.10 g (0.08 mmol) of the G3 dendron, 0.014 g (0.12 mmol) of DABCO, and 0.05 mL (0.5 mmol) of $TiCl_4$. The product was isolated by silica gel column chromatography using from 12:2:3 to 3:1:1 hexane/ethyl acetate/chloroform with 2% Et_3N as the eluent, yielding 0.095 g (89%). ^1H NMR (400 MHz, $CDCl_3$, TMS standard, 20 °C, ppm) δ 7.72 (s, 8H), 7.54–7.12 (m, 37H), 7.03–6.49 (m, 24H); ^{13}C NMR (100 MHz, $CDCl_3$, TMS standard, 20 °C, ppm) δ 168.91, 168.78, 168.41, 168.17, 168.11, 167.63, 153.91, 153.63, 151.83, 151.71, 151.53, 139.23, 139.08, 135.75, 135.61, 135.55, 134.26, 134.12, 132.33, 130.88, 130.80, 130.60, 130.53, 130.37, 130.22, 130.05, 129.94, 129.78, 129.62, 129.35, 129.09, 128.72, 128.38, 128.16, 127.98, 127.83, 127.76, 122.78, 121.26, 120.79, 120.73, 120.48, 120.24, 120.09; MALDI-TOF-Mass: 1331.1 ($[M]^+$ Calcd for $C_{97}H_{70}N_7$: 1331.6); Anal. Calcd for $C_{97}H_{69}N_7$: C, 87.42; H, 5.22; N, 7.36%. Found: C, 87.49; H, 5.21; N, 7.35%.

Half-DPA-H G4: The previous procedure was followed using 0.02 mL (0.19 mmol) of aniline, 0.05 g (0.02 mmol) of the G4 dendron, 0.014 g (0.12 mmol) of DABCO, and 0.05 mL (0.5 mmol) of $TiCl_4$. The product was isolated by silica gel column chromatography using from 6:1:6 to 3:1:3 hexane/ethyl acetate/chloroform with 2% Et_3N as the eluent, yielding 0.044 g (80%). ^1H NMR (400 MHz, $CDCl_3$, TMS standard, 20 °C, ppm) δ 7.76–6.37 (m, 141H); ^{13}C NMR (100 MHz, $CDCl_3$, TMS standard, 20 °C, ppm) δ 168.80, 168.35, 168.06, 154.03, 153.62, 151.77, 146.62, 139.14, 138.93, 138.79, 137.39, 135.65, 135.44, 134.24, 132.38, 132.25, 130.79, 130.46, 130.23, 129.97, 129.89, 129.27, 128.71, 128.28, 128.07, 127.89, 127.73, 120.72, 120.40, 120.16, 119.88, 119.67; MALDI-TOF-Mass: 2763.92 ($[M]^+$ Calcd for $C_{201}H_{141}N_{15}$: 2764.15); Anal. Calcd for $C_{201}H_{141}N_{15}$: C, 87.27; H, 5.14; N, 7.59%. Found: C, 87.22; H, 5.18; N, 7.51%.

Half-DPA-MeO G4: The previous procedure was followed using 0.023 g (0.19 mmol) of methoxyaniline, 0.05 g (0.02 mmol) of the G4 dendron, 0.014 g (0.12 mmol) of DABCO, and 0.05 mL (0.5 mmol) of $TiCl_4$. The product was isolated by silica gel column chromatography using from 6:1:6 to 3:1:3 hexane/ethyl acetate/chloroform with 2% Et_3N as the eluent, yielding 0.045 g (81%). ^1H NMR (400 MHz, $CDCl_3$, TMS standard, 20 °C, ppm) δ 7.76–6.40 (m, 143H); ^{13}C NMR (100 MHz, $CDCl_3$, TMS standard, 20 °C, ppm) δ 168.02, 167.05, 167.56, 153.08, 153.01, 151.57, 145.12, 139.04, 138.93, 138.74, 137.43, 135.65, 135.42, 134.14, 132.28, 132.05, 130.69, 130.16, 130.22, 129.96, 129.81, 129.26, 128.70, 128.22, 128.01, 127.69, 127.67, 120.62, 120.10, 120.11, 119.87, 119.63; MALDI-TOF-Mass: 2795.00 ($[M]^+$ Calcd for $C_{202}H_{143}N_{15}$: 2794.16); Anal. Calcd for $C_{202}H_{143}N_{15}O$: C, 86.76; H, 5.15; N, 7.51%. Found: C, 86.69; H, 5.18; N, 7.52%.

Half-DPA-Cl G4: The previous procedure was followed using 0.024 g (0.19 mmol) of chloroaniline, 0.05 g (0.02 mmol) of the G4 dendron, 0.014 g (0.12 mmol) of DABCO, and 0.05 mL (0.5 mmol) of $TiCl_4$. The product was isolated by silica gel column chromatography using from 6:1:6 to 3:1:3 hexane/ethyl acetate/chloroform with 2% Et_3N as the eluent, yielding 0.044 g (79%). ^1H NMR (400 MHz, $CDCl_3$, TMS standard, 20 °C, ppm) δ 7.74–6.43 (m, 140H); ^{13}C NMR (100 MHz, $CDCl_3$, TMS standard, 20 °C, ppm) δ 168.92, 168.55, 168.21, 154.63, 153.92, 151.68, 146.42, 139.06, 138.23, 138.88, 137.19, 135.44, 135.40, 134.14, 132.18, 132.11, 130.75, 130.41, 130.00, 129.97, 129.89, 129.17, 128.67, 128.28, 128.06, 127.77, 127.41, 120.71, 120.39, 120.06, 119.61, 119.49; MALDI-TOF-Mass: 2799.02 ($[M]^+$ Calcd for $C_{201}H_{140}ClN_{15}$: 2798.11); Anal. Calcd for $C_{201}H_{140}ClN_{15}$: C, 86.19; H, 5.04; N, 7.50%. Found: C, 86.57; H, 5.08; N, 7.56%.

Half-DPA-CF_3 G4: The previous procedure was followed using 0.031 g (0.19 mmol) of 2-(trifluoromethyl)aniline, 0.05 g (0.02 mmol) of the G4 dendron, 0.014 g (0.12 mmol) of DABCO, and 0.05 mL (0.5 mmol) of $TiCl_4$. The product was isolated by silica gel column chromatography using from 6:1:6 to 3:1:3 hexane/ethyl acetate/chloroform with 2% Et_3N as the eluent, yielding 0.044 g (78%). ^1H NMR (400 MHz, $CDCl_3$, TMS standard, 20 °C, ppm) δ 7.82–6.42 (m, 140H); ^{13}C NMR (100 MHz, $CDCl_3$, TMS standard, 20 °C, ppm) δ 169.80, 169.35, 168.76, 154.01, 153.42, 151.67, 146.61, 139.10, 138.83, 138.66, 137.38, 135.65, 135.41, 134.14, 132.28, 132.05, 130.70, 130.42, 130.22, 129.97, 129.89, 129.17, 128.69, 128.29, 128.02, 127.89, 127.73, 120.71, 120.33, 120.18, 119.86, 119.66; MALDI-TOF-Mass: 2833.10 ($[M]^+$ Calcd for $C_{202}H_{140}F_3N_{15}$: 2763.76).

Calculation of the Equilibrium and Isosbestic Point in UV–Vis Spectra. The equilibrium constants of the coordination (Eqs. 1–4) are defined as K_a–K_d for imines in each generation. The values of K_N are given by layers:

$$K_N = \frac{[NH^+]}{[N][H^+]}: \quad (N = A\text{–}D). \tag{5}$$

Equation 5 leads to

$$[N] = \frac{[N]_0}{K_N[H^+] + 1} \tag{6}$$

using the relation of $[N] + [NH^+] = [N]_0$ (N = A, B, C, and D) where $[A]_0$, $[B]_0$, $[C]_0$, and $[D]_0$, represent the initial concentrations of A, B, C, and D, respectively. $[H^+]$ is represented by using the concentration of the unprotonated imines ([A], [B], [C], and [D]): and their initial concentrations:

$$\begin{aligned}[H^+] &= [H^+]_0 - [AH^+] - [BH^+] - [CH^+] - [DH^+] \\ &= [H^+]_0 - ([A]_0 - [A]) - ([B]_0 - [B]) \\ &\quad - ([C]_0 - [C]) - ([D]_0 - [D]).\end{aligned} \tag{7}$$

Substituting (6) into (7) yields the equation for $[H^+]$, K_N, and $[N]_0$. We can calculate the concentrations of each chemical species ($[H^+]$, [N], and $[NH^+]$ for N = A–D) after the equilibrium on the basis of (6) and (7) by four given (or assumed) K_N values,

because the initial concentrations $[H^+]_0$ and $[N]_0$ are known constants.

To determine accurate constants of the complexation, we have to know the concentration profiles on the addition of H^+. In general, it is impossible to determine the discrete information about concentrations from a titration curve (absorption changes vs molar amounts) in a multi-equilibrium system. If the absorption spectra changes corresponding to each equilibrium reaction are well-separated, we can determine by the titration curve fitting at some different wavelengths. However, in our case, it is impossible because the spectral difference between complexations at each layer of **Half-DPA** is very small. Thus, we tried to analyze the isosbestic points during the titration.

The UV–vis absorption coefficient is expressed as a function of the Gaussian type for the wavenumber. Therefore, the function for the wavelength is given by:

$$\varepsilon(\lambda) = \varepsilon^0 \exp\left\{\frac{-\delta(1/\lambda^0 - 1/\lambda)^2}{kT}\right\} \tag{8}$$

where λ^0 is the wavelength of maximum absorption, ε^0 is the molar absorption coefficient for λ^0, and δ is the thermal vibration parameter of the chromophore. Here, we assume the δ value to be constant ((kT/δ) to be 10^7 nm^2) for each chromophore because the influence to the wavelength of the isosbestic point is very small. In this case, these chromophores are at each imine site and are influenced by the protonation. The overall absorption can be expressed as the summation of Eq. 8 for each chromophore (A–D and AH^+–DH^+) based on the approximation that no interaction is present between neighboring chromophores.

$$\mathrm{Abs}(\lambda, [H^+]) = \sum_{N}^{A\to D} [N]\varepsilon_N^0 \exp\left\{\frac{-\delta_N(1/\lambda_N^0 - 1/\lambda)^2}{kT}\right\} + [NH]\varepsilon_{NH}^0 \exp\left\{\frac{-\delta_{NH}(1/\lambda_{NH}^0 - 1/\lambda)^2}{kT}\right\}. \tag{9}$$

The wavelength of the isosbestic point, λ_{iso}, is a solution of the following equation for λ, because the λ_{iso} is defined as the wavelength where the absorbance does not change upon titration.

$$\mathrm{Abs}(\lambda_{iso}, [H^+] + \Delta[H^+]) - \mathrm{Abs}(\lambda_{iso}, [H^+]) = 0. \tag{10}$$

The variation of isosbestic points for the concentration of added H^+ ($[H^+]_0$) can be calculated by solving Eq. 10 when the various λ^0, ε^0, and K_N values are defined. The λ^0 and ε^0 are obtained from the differential spectra during the titration experiment. In principle, the K_N values were estimated by fitting the theoretical λ_{iso} profiles into the experiment. However, this procedure was not sufficient to obtain the absolute values of K_N, although the relative values among the K_a–K_d could be estimated. The absorbance profiles during the titration should be employed with analysis of the isosbestic point to calculate the exact coordination constants. They are also expressed as Eq. 9.

These methods are not only applicable for the protonation, but also the 1:1 complexation of a Lewis acid (e.g., $SnCl_2$) to the imines.

This work was partially supported by CREST from the Japan Science and Technology Agency, Grants-in-Aid for Scientific Research (Nos. 15036262, 15655019, 15350073) and the 21st COE program (KEIO-LCC) from the Ministry of Education, Culture, Sports, Science and Technology.

References

1 For reviews, see: a) J. M. J. Fréchet and D. A. Tomalia, "Dendrimers and Other Dendritic Polymers," J. Wiley and Sons, New York (2001). b) G. R. Newkome, C. N. Moorefield, and F. Vögtle, "Dendritic Molecules: Concept, Synthesis, Perspectives," Wiley-VCH, Weinheim (1996).

2 a) C. Devadoss, P. Bharathi, and J. S. Moore, *J. Am. Chem. Soc.*, **118**, 9635 (1996). b) D. L. Jiang and T. Aida, *Nature*, **388**, 454 (1997). c) T. D. Selby and S. C. Blackstock, *J. Am. Chem. Soc.*, **120**, 12155 (1998).

3 a) C. W. Tang and S. A. VanSlyke, *Appl. Phys. Lett.*, **51**, 913 (1987). b) U. Bach, D. Lupo, P. Comte, J. E. Moser, F. Weissörtel, J. Salbeck, H. Spreitzer, and M. Grätzel, *Nature*, **395**, 583 (1998).

4 a) P. Furuta, J. Brooks, M. E. Thompson, and J. M. J. Fréchet, *J. Am. Chem. Soc.*, **125**, 13165 (2003). b) B. Li, J. Li, Y. Fu, and Z. Bo, *J. Am. Chem. Soc.*, **126**, 3430 (2004).

5 a) K. Yamamoto, M. Higuchi, S. Shiki, M. Tsuruta, and H. Chiba, *Nature*, **415**, 509 (2002). b) T. Imaoka, H. Horiguchi, and K. Yamamoto, *J. Am. Chem. Soc.*, **125**, 340 (2003). c) N. Sato, J.-S. Cho, M. Higuchi, and K. Yamamoto, *J. Am. Chem. Soc.*, **125**, 8104 (2003). d) M. Higuchi, M. Tsuruta, H. Chiba, S. Shiki, and K. Yamamoto, *J. Am. Chem. Soc.*, **125**, 9988 (2003).

6 a) B. Karakaya, W. Claussen, K. Gessler, W. Saenger, and A. D. Schlüter, *J. Am. Chem. Soc.*, **119**, 3296 (1997). b) T. Sato, D.-L. Jiang, and T. Aida, *J. Am. Chem. Soc.*, **121**, 10658 (1999). c) S. Setayesh, A. C. Grimsdale, T. Weil, V. Enkelmann, K. Müllen, F. Meghdadi, E. J. W. List, and G. Leising, *J. Am. Chem. Soc.*, **123**, 946 (2001). d) A. Kimoto, K. Masachika, J.-S. Cho, M. Higuchi, and K. Yamamoto, *Org. Lett.*, **6**, 1179 (2004). e) A. Kimoto, K. Masachika, J.-S. Cho, M. Higuchi, and K. Yamamoto, *Chem. Mater.*, **16**, 5706 (2004).

7 a) W. Guo, J. J. Li, Y. A. Wang, and X. Peng, *J. Am. Chem. Soc.*, **125**, 3901 (2003). b) F. Le Derf, E. Levillain, G. Trippe, A. Gorgues, M. Salle, R. M. Sebastian, A. M. Caminade, and J. P. Majoral, *Angew. Chem., Int. Ed.*, **40**, 224 (2001). c) H. C. Yoon and H. S. Kim, *Anal. Chem.*, **72**, 922 (2000).

8 a) M. Higuchi, S. Shiki, and K. Yamamoto, *Org. Lett.*, **2**, 3079 (2000). b) M. Higuchi, S. Shiki, K. Ariga, and K. Yamamoto, *J. Am. Chem. Soc.*, **123**, 4414 (2001).

9 Complexation of $SnCl_2$ with imines, see: J. M. Van den Berg, *Acta Crystallogr.*, **15**, 1051 (1962).

10 These complexation behaviors were the same as the di-substituted phenylazomethine dendrimers (previous study) based on the same chemical shifts attributed to the imine carbon for each generation. These results suggested that, for these dendrimers, there is no steric influence on the morphology of the dendrimers substituted by one and two dendrons, complexing with $SnCl_2$.

11 These differences are based on their unique dendritic layers and the structural vectors of the imine bond. From outer layers, imine nitrogen acts as electron-donating substituents, whereas from inner layers, imine carbon acts as electron-withdrawing ones. As a result of the summation of electronic donation/acceptance, the stepwise sequence of the basicity on the phenylazomethine dendron could be realized.